

## METHODS

# Distribution Density-Aware Compensation for High-Resolution Stretchable Display

SUNG-HOON JUNG, JUNG-HYUN KIM<sup>1</sup>, AND SUK-JU KANG<sup>1</sup>, (Member, IEEE)

Department of Electronic Engineering, Sogang University, Seoul 04107, South Korea

Corresponding author: Suk-Ju Kang (sjkang@sogang.ac.kr)

This work was supported by the National Research Foundation of Korea (NRF) grant funded by the Korea government (MSIT) (No. 2020M3H4A1A02084899).

**ABSTRACT** When a stretchable display is stretched, the area of the exposed substrate between the light-emitting diodes (LEDs) increases, decreasing the image luminance. Currently, this problem is not addressed in existing high-resolution display systems. Although the mean-based method and gamma correction method using general image processing techniques, which are first presented in this paper, can compensate for the decrease in luminance, these methods cannot be adaptively applied for stretchable display systems. Therefore, this paper proposes a novel image compensation method optimized for stretchable displays. The proposed distribution density-aware method (DDAM) compensates for the decrease in luminance particularly for the area involving the newly exposed substrate. The DDAM solves the saturation problem associated with the mean-based method and the problem of inaccurate luminance estimation associated with the gamma correction method. Compared with the mean-based method and the gamma correction method, the peak signal-to-noise ratio of the DDAM is 0.600 dB and 1.977 dB higher, respectively. The structural similarity index measure is also 0.055 and 0.057 higher, respectively. In addition, we develop a novel simulator to evaluate the stretching of high-pixel-per-inch displays, which are being actively researched, and use it to verify the performance of above mentioned luminance reduction compensation methods.

**INDEX TERMS** Stretchable display, luminance compensation, simulator, point spread function.

## I. INTRODUCTION

The increased user demand for different types of displays in addition to the development of display technologies has accelerated the research on stretchable displays characterized by display substrates that can be stretched [1]–[3]. In such displays, the display size is varied by stretching the device and adjusting the space between pixels. Displays can be stretched using structural and material stretching methods [4]–[7]. In structural stretching methods, the distance between the light-emitting diodes (LEDs) in a device is increased by modifying the structure of the device, for instance, by incorporating origami and kirigami structures [8]–[12], wavy structures [13]–[17], and island-bridge structures [18]–[21]. Origami and kirigami structures form a net through the folding or cutting of a planar substrate and deform in three dimensions when a force is applied. Wavy structures exhibit

stretching characteristics owing to the corrugated shape of the substrate. Island-bridge structures exhibit stretching characteristics by forming a connection between the LEDs in a bent shape. Material stretching methods are aimed at developing devices that are stable, flexible, and self-stretchable without structural deformation. Typical flexible devices include stretchable transparent electrodes [4], [22]–[24], thin-film transistors [25], [26], and LEDs [27]–[29]. Stretchable transparent electrodes consist of a nanowire transparent device with high conductivity and elasticity. Stretchable thin-film transistors use carbon nanotubes and ion gels to provide the voltage and current required for powering LEDs. Stretchable LEDs involve a composite material obtained by combining phosphor particles and an elastomer matrix, which emits light even when stretched.

Regardless of the type of stretching method used, the distance between the LEDs increases when a display is stretched, and thus, the display substrate between the LEDs is exposed. This defect must be compensated for because the stretched

The associate editor coordinating the review of this manuscript and approving it for publication was Senthil Kumar<sup>1</sup>.

output image may be distorted, and a zero-luminance pattern may be observed between the LEDs.

More specifically, this defect must be evaluated through human visual perception and solved from a cognitive perspective. The human eye perceives a point light source as a diffraction pattern, such as an airy disk, which has a bright part in the center and bright and dark rings that alternate around the center. In a display, the human eye recognizes light from LEDs as blurred profile, which varies with the viewing distance. Owing to this blurred recognition of the LED light, a zero-luminance pattern between the LEDs may reduce the luminance. The mean-based method and gamma correction method for general image processing techniques, which will be first presented in the next section, can compensate for the luminance reduction. In particular, the mean-based method compensates for the reduction in luminance in proportion to the average luminance change ratio of the image. The gamma correction method implements nonlinear compensation for the luminance reduction. Notably, because these methods perform luminance compensation without considering the zero-luminance pattern between LEDs, the pixels of the newly exposed substrate can still be observed. To address this limitation, this paper proposes a novel method of luminance compensation optimized for stretchable displays, called the distribution density-aware method (DDAM). The DDAM concentrates the compensation on the pixels around the exposed substrate. When the point spread function (PSF), which indicates the optical recognition of a point light source, is applied, the zero-luminance pattern appears faded, thereby generating natural images.

The existing stretchable display technologies exhibit the limitations of conductivity disconnection and resistance for high pixel-per-inch (PPI) scenarios. Most of the existing studies address the luminance decrease problem only for low-PPI displays [30], [31]. Therefore, a simulator must be developed to perform luminance compensation tests on stretchable displays with a high PPI. To this end, we have created a novel simulator that can perform experiments on image compensation with different stretch ratios, viewing distances, and compensation methods. To incorporate human cognition in the simulator, we developed a retina model based on the PSF. The retina model determines the sigma of the PSF, which regulates the degree of blur, according to the viewing distance. The contributions of this research can be summarized as follows:

■ We created a novel simulator that can perform comparative experiments with different stretch ratios, viewing distances, and compensation methods for high-PPI stretchable displays to be further developed in the future.

■ To solve the problem of luminance reduction in high-PPI stretchable displays, we considered the mean-based method and gamma correction method based on general image processing methods. Additionally, we propose a novel method, the DDAM, to address the zero-luminance pattern caused by the exposed substrate from a cognitive perspective.

■ To adjust the human optical recognition of LED light according to the viewing distance, we propose a retina model that can determine the degree of blur size using the PSF. The compensated images processed using the retina model are compared in terms of the peak signal-to-noise ratio (PSNR) and structural similarity index measure (SSIM).

## II. RELATED WORK

With advancements in display technologies and the growth of the application field of displays, the demand for flexible displays has increased. Flexible displays can be categorized into foldable, rollable, and stretchable displays. These display types are introduced in the following sub-sections.

### A. FOLDABLE DISPLAY

A foldable display can be folded and unfolded by replacing the glass substrate of existing rigid displays with a substrate composed of a flexible material such as a plastic or a thin glass substrate and decreasing the radius of curvature [32]–[34]. When physical stress due to continuous deformation is applied to the substrate, fracture or delamination associated with the cracking of the substrate may occur [35]. In addition, the physical stress is typically concentrated around the folding region. Therefore, durability must be ensured when developing foldable display technologies.

### B. ROLLABLE DISPLAY

A rollable display implements deformation using a flexible glass substrate material that can be rolled similarly to a tissue roll. Such displays boast high portability because a rollable display can be unrolled and used when necessary and rolled when stored. Because rolling-type deformation is implemented, the curvature radius is not as limited as in the case of a foldable display. However, a rollable display is unstable when exposed to a hot or humid environment [36]. In addition, because the entire panel area is rolled, the overall physical stress must be considered. To develop rollable display technologies, a large number of rollable parts must be introduced, and natural rolling characteristics must be ensured.

### C. STRETCHABLE DISPLAY

A stretchable display is a free-form display, which is the final expected form of a flexible display. Firstly, durability must be ensured for stretchable displays because when the components are stretched to several times the original dimensions to achieve a large deformation and exposed to a severe physical and chemical environment, physical erosion and dysfunction may occur [37]. Secondly, strain reversibility must be ensured to allow the display to be freely deformed while restoring the substrate to a flat state even when the display has been deformed for a considerable period [38]. Stretchable displays can be implemented using material or structural stretching methods. Both these stretching methods lead to image distortion. To address image distortion, we have developed a novel compensation method.

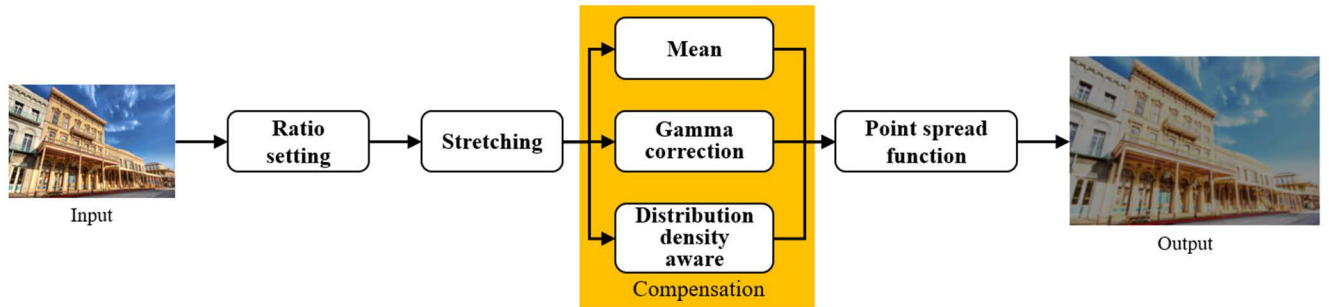


FIGURE 1. Overall block diagram for the proposed simulator.

### III. PROPOSED SIMULATOR

We have created a novel simulator to perform experiments with a high-PPI display. The simulator can create images that are stretched according to a specific stretch ratio and perform image compensation using the mean-based method, gamma correction method, or the DDAM. The simulator enables the comparative analysis of these three methods. Furthermore, to evaluate the optical recognition results based on human perception, an image is generated with the PSF. Fig. 1 shows the functional block diagram for the proposed simulator and a sample result image.

#### A. STRETCHING OPERATION

In a stretchable display, the width and height of the exposed display substrate vary depending on the stretch ratio. Hence, the amount of luminance reduction in the stretched image changes with respect to the stretch ratio. Therefore, the simulator is designed to implement stretching and compare the performance of the three previously mentioned methods. The simulator implements a newly exposed substrate between the LEDs by inserting black pixels for each predetermined number of pixels. One black pixel, represented by a hole with no light emission, is inserted per 9 pixels, 5 pixels, and 3 pixels to output 11%, 20%, and 30% stretched images, respectively. Stretched images are generated by inserting empty pixels between the image pixels according to the stretch ratio.

#### B. COMPENSATION

The decrease in luminance due to stretching can be compensated for by using several methods, which are incorporated in the simulator. Specifically, compensated images are generated using either the mean-based method or the gamma correction method, which are based on general image processing methods, or the DDAM, which is the presented novel method optimized for stretchable displays.

##### 1) MEAN-BASED METHOD

The mean-based method aims to maintain the average luminance of an image. All the pixels of a stretched image are multiplied by the same factor such that the average luminance is equivalent to the ground truth image. The multiplication factor is the ratio of the luminance of the stretched image

to that of the original image. The mean-based method can maintain luminance through a simple operation. However, because the luminance is compensated for by a specific ratio without considering the intensity of each pixel, saturation may occur in high-luminance scenarios in which the pixel value exceeds the maximum value of the dynamic range. The mean-based method can be modeled as follows:

$$V_{mean} = \frac{\sum I_{groundtruth}(x, y)}{\sum I_{previous}(x, y)}, \quad (1)$$

$$I_{compensated}(x, y) = V_{mean} \times I_{previous}(x, y), \quad (2)$$

where  $I_{previous}$  is the luminance of the image before it is stretched,  $I_{groundtruth}$  is the luminance of the ground truth image, and  $I_{compensated}$  is the luminance of the compensated image. The ground truth is the image interpolated by bilinear interpolation for a zero-luminance pattern, which is caused by the area increase of exposed substrate between the LEDs.

##### 2) GAMMA CORRECTION METHOD

According to Weber's law, the human eye reacts nonlinearly to luminance. For example, if the luminance of an image increases linearly, the luminance will not appear to be smooth because the human eye perceives artifacts through an inherent vision mechanism. The gamma correction method compensates for the luminance to reflect human optical properties and increases the luminance in a nonlinear manner. Specifically, this method compensates for the luminance with an exponential value for the normalized luminance of the input image. Saturation does not occur because intensive compensation is performed for intermediate luminance, and moderate compensation is performed for low and high luminance. The gamma correction method can be modeled as follows:

$$I_{compensated}(x, y) = 255 \left( \frac{I_{previous}(x, y)}{255} \right)^{\frac{1}{\gamma}}, \quad (3)$$

where  $I_{previous}$  is the luminance of the image before being stretched, and  $I_{compensated}$  is the luminance of the compensated image.

##### 3) DDAM

In the mean-based method and gamma correction method, the extent of luminance compensation is determined by the

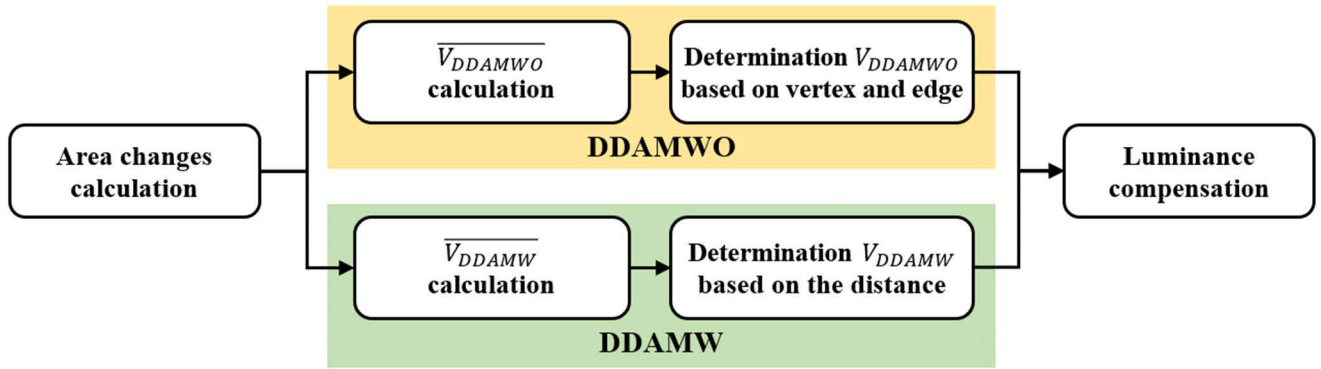


FIGURE 2. Overall block diagram of the DDAM using the DDAMWO and DDAMW.

luminance value, and the newly exposed substrate is not considered. Consequently, when these two methods are applied to a stretchable display, insufficient compensation may occur in terms of the PSF. Therefore, we propose the DDAM, which compensates for the decrease in luminance in the form of an inverse Gaussian filter for each LED, considering the exposed area of the substrate. Fig. 2 presents the overall block diagram of the DDAM. First, the DDAM calculates the changes in the area caused by the newly exposed substrate. Specifically, if the areas of the original and stretched images are  $S$  and  $S'$ , respectively, the change in the area is  $(S' - S)$ , corresponding to a pixel number of  $2R + 1$ . Second, the luminance compensation multiplier is manually determined considering the newly exposed substrate. When the pixel is near or far from the newly exposed substrate, the multiplier is increased or decreased, respectively. In this manner, the decrease in luminance is compensated for considering the area according to the stretch ratio. The DDAM consists of two methods that differ in terms of the distance consideration. In the DDAM without distance consideration (DDAMWO), the pixels adjacent to the exposed substrate are weighted. The number of pixels adjacent to the exposed substrate is  $4(R - 1)$ . In the DDAM with distance consideration (DDAMW), all pixels are weighted with respect to the distance from the exposed substrate. Therefore, the number of compensated pixels is  $R^2$ . The formulas for the DDAMWO and DDAMW are as follows:

$$\overline{V_{DDAMWO}} = \frac{2R + 1}{4(R - 1)}, \quad (4)$$

$$\overline{V_{DDAMW}} = \frac{2R + 1}{R^2}, \quad (5)$$

where  $R$  denotes the stretch ratio and  $\overline{V_{DDAMWO}}$  and  $\overline{V_{DDAMW}}$  represent the mean of the DDAMWO's luminance compensation multipliers  $V_{DDAMWO}$  and the DDAMW's luminance compensation multipliers  $V_{DDAMW}$ , respectively. We manually determine  $V_{DDAMWO}$  based on the vertex and edge and  $V_{DDAMW}$  based on the distance from the pixel of the exposed substrate. The  $V_{DDAMWO}$  values of the pixels located at the vertex and edge are large and small, respectively. The

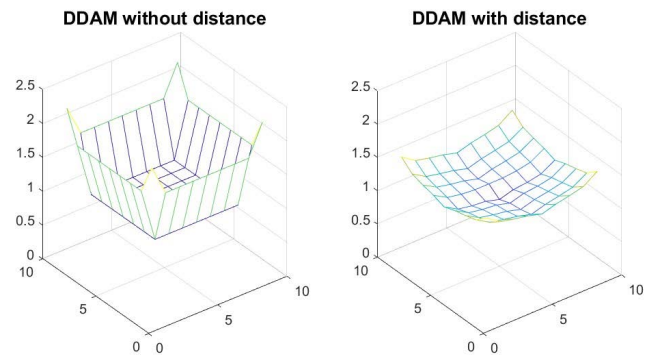


FIGURE 3. Multipliers of the DDAMWO and DDAMW for a stretch ratio of 11%. The units of the x-axis and y-axis are pixels.

$V_{DDAMW}$  values of the pixels farther from the exposed area of the substrate are smaller. The DDAMW involves small compensation multipliers and has a smoother form because the number of pixels being compensated is greater than that in the DDAMWO. Fig. 3 shows the forms of the DDAMWO and DDAMW when the stretch ratio is 11%. The compensation multipliers for both methods are small at the center and large at the edge, similar to an inverse Gaussian filter. Therefore, the negative effects of the newly exposed substrate are counterbalanced and blurred when the optical properties are applied through the PSF.

### C. RETINA MODEL APPLICATION

The human eye focuses the light reflected by an object onto the retina by adjusting the cornea and pupil sizes. The human eye perceives an object as the light source unit of a diffraction pattern, such as an airy disk, rather than a point light source when the object is located near or far from the best focus location. According to Rayleigh's criterion, which indicates the condition for distinguishing two point light sources when the diffraction patterns of the air disks for the two sources overlap, the blur size can be determined by the distance from the best focus [39], [40]. Therefore, the simulator is designed to adjust the PSF according to the viewing distance through the retina model. Fig. 4 schematically illustrates the retina

**TABLE 1.** Performance comparison of the luminance compensation methods at different stretch ratios and relative distances. The boldfaced values indicate the best values.

Stretch ratio	Relative distance	PSNR (dB) / SSIM			
		Mean-based	Gamma correction	DDAMW	DDAMWO
11%	2	16.845 / 0.553	16.605 / 0.538	17.644 / 0.586	<b>18.294 / 0.615</b>
	3	18.081 / 0.586	17.488 / 0.569	19.082 / 0.631	<b>19.659 / 0.676</b>
	4	18.506 / 0.596	17.762 / 0.579	19.527 / 0.644	<b>19.923 / 0.688</b>
20%	2	15.169 / 0.449	14.526 / 0.451	15.879 / 0.493	<b>16.160 / 0.509</b>
	3	16.808 / 0.508	15.365 / 0.507	17.533 / 0.562	<b>17.617 / 0.586</b>
	4	17.441 / 0.533	15.634 / 0.530	<b>18.055 / 0.584</b>	17.976 / <b>0.604</b>
33%	2	13.966 / 0.397	12.582 / 0.416	<b>14.365 / 0.438</b>	14.279 / <b>0.462</b>
	3	15.737 / 0.505	13.167 / 0.512	<b>15.740 / 0.539</b>	15.208 / <b>0.558</b>
	4	16.255 / 0.553	13.293 / 0.555	<b>16.083 / 0.580</b>	15.397 / <b>0.593</b>
Avg.		16.534 / 0.520	15.158 / 0.517	17.101 / 0.562	<b>17.168 / 0.588</b>

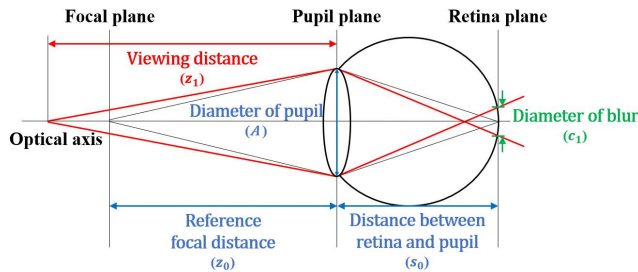


**FIGURE 4.** Schematic of the retina model.  $z_0$  is the reference focal distance, and  $s_0$  is the distance between the retina and pupil. The viewing distance  $z_1$  determines the diameter of blur  $c_1$ , given the diameter of pupil,  $A$ .

model. The blur diameter can be calculated according to the viewing distance. When the cornea and pupil are fixed, the perceived image appears blurred depending on the distance from the reference focal distance. The following equations define the diameter of blur  $c_1$  and relative distance  $L$ :

$$c_1 = A \frac{s_0}{z_0} \left| 1 - \frac{1}{L} \right|, \tag{6}$$

$$L = \frac{z_0}{z_1}, \tag{7}$$

where  $A$  denotes the pupil diameter,  $s_0$  is the distance between the retina and pupil, and  $z_0$  and  $z_1$  represent the reference focal distance and viewing distance, respectively.

**D. SIMULATOR GRAPHICAL USER INTERFACE (GUI)**

We have designed a simulator to perform high-PPI image experiments through a GUI, as shown in Fig. 5. The GUI includes three stretch ratios to compare the compensation method performances at different stretch ratios. Moreover, the PSF can be modified to consider the relative distance according to the viewing distance. This GUI can be used to quantitatively evaluate the performance of the different

methods through the PSNR and SSIM and visually evaluate the performance through the compensated images.

**IV. EXPERIMENTAL RESULTS**

We performed experiments with four types of luminance compensation methods: the mean-based method, gamma correction method, DDAMW, and DDAMWO. In the experiments for each method, the stretch ratio was changed from 11% to 33%, and the relative distance was changed from 2 to 4. Considering the ordinary case of people using a computer, the relative distance was set as 1 when the viewing distance was 24 inches, and the image was precisely focused [41], [42]. Because we needed an image for high-PPI displays as the target application of the simulator, the Urban100 dataset [43], which is widely used in super-resolution applications, was adopted. For the gamma correction method,  $\gamma$  was set to 1.2 since it yields the highest performance, as determined experimentally.

**A. LUMINANCE COMPENSATION PERFORMANCE**

To evaluate the performance of the luminance compensation methods, nine experiments were conducted with stretch ratios of 11%, 20%, and 33% and relative distances of 2, 3, and 4. Table 1 summarizes the PSNR and SSIM values for all combinations. In terms of the PSNR, the gamma correction method exhibited the lowest performance (15.158 dB), followed by the mean-based method (16.534 dB, which is 1.376 dB higher than the results of the gamma correction method). The proposed DDAMW achieved a PSNR of 17.101 dB, which is 0.567 dB higher than that of the mean-based method. The proposed DDAMWO exhibited a PSNR of 17.168 dB, which is 0.067 dB higher than that of the DDAMW, and outperformed the other methods. The trends for the SSIM were similar to those of the PSNR. The performance comparison in terms of the PSNR and SSIM indicated that the images were naturally compensated from best to worst in the order

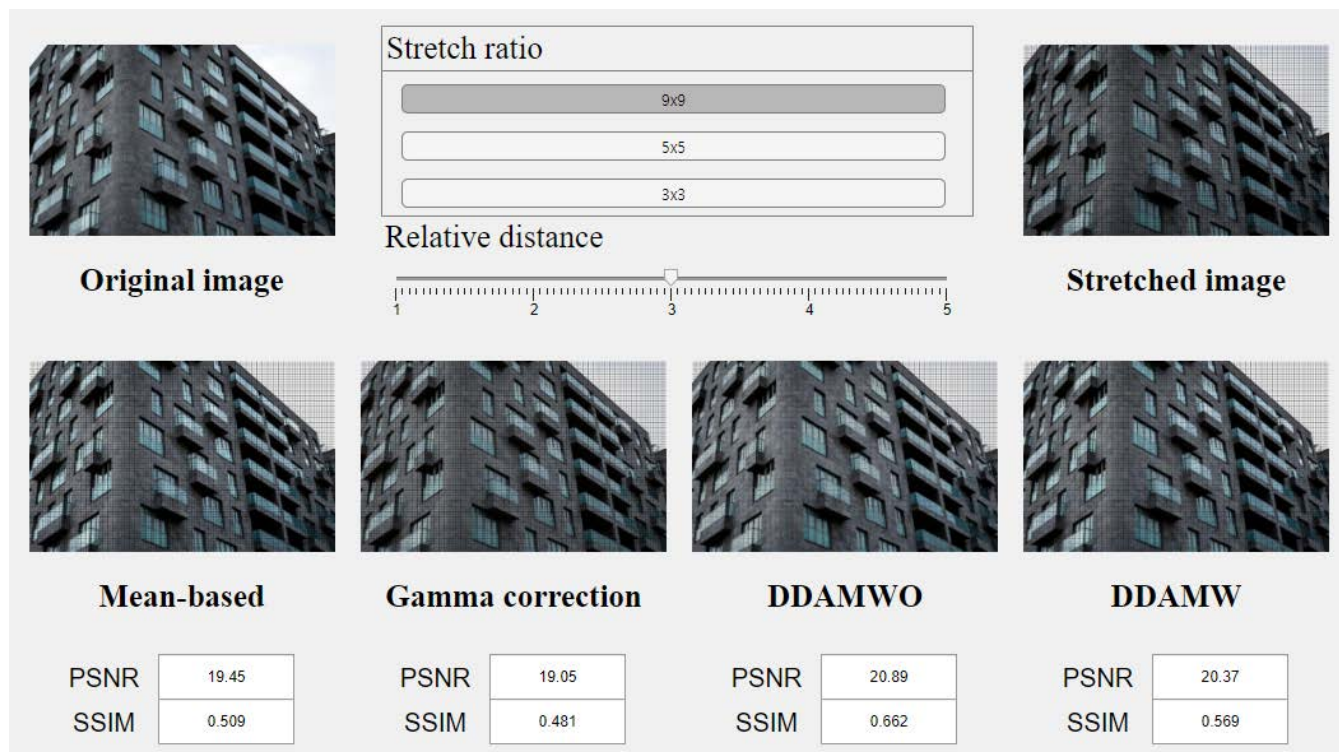


**FIGURE 5.** Graphical user interface (GUI) of the simulator for luminance compensation. The GUI consists of the controllers for the stretch ratio and relative distance, an input image, a stretched image, and images compensated by each luminance compensation method. The GUI represents the performance of each compensated image in terms of the PSNR and SSIM.

of DDAMWO, DDAMW, mean-based method, and gamma correction method. Because the gamma correction method used a fixed parameter  $\gamma$ , the extent of luminance compensation was the same for all stretch ratios. Therefore, the gamma correction method always exhibited the most inferior performance, and the performance degradation intensified as the stretch ratio increased. Because the mean-based method aimed at maintaining the average luminance, the compensation multipliers changed with the stretch ratio. Therefore, this method outperformed the gamma correction method by achieving a similar luminance as that of the original image. However, because one specific multiplier increased all pixel values, high pixel intensities were often saturated to the maximum pixel intensity values, and the saturation occurred more frequently as the stretch ratio increased. Therefore, the DDAM, which compensates for the decreased luminance by adjusting the pixels by using different multipliers, achieved higher quality images than those obtained using the mean-based method. The DDAMW was expected to outperform the DDAMWO. However, in the experiment, the DDAMWO exhibited a higher PSNR and provided a better luminance compensation performance than the DDAMW. Because the DDAMWO adjusted the pixels adjacent to the exposed substrate by using higher multipliers than those of the DDAMW, the application of the PSF provided the most appropriate compensation around the exposed substrate. Because the DDAMW used lower multipliers, it could not sufficiently

compensate for the zero-luminance pattern. Therefore, the performance was higher when the distance was not considered. Fig. 6 shows the full size, patch size images, and patch size heatmap for the compensated images and images applied PSF. This figure shows that the newly exposed substrate of the DDAMWO and DDAMW is faded compared with the exposed substrate of the mean-based method and gamma correction method.

### B. STRETCH RATIOS

To compare the performance of the methods at different stretch ratios, experiments were performed with stretch ratios of 11%, 20%, and 33%. When the stretch ratio was 11% or 20%, the performance order of the compensation methods was the same. Specifically, the luminance decrease was sufficiently compensated for by the best to worst methods in the order of DDAMWO, DDAMW, mean-based method, and gamma correction method. Because the gamma correction method could not consider the stretch ratio, the amount of luminance compensation was the same for all stretch ratios. Therefore, the gamma correction method exhibited the lowest performance. Moreover, as the stretch ratio increased, the luminance compensation multiplier  $V_{mean}$  increased; thus, the saturation problem occurred more frequently. Consequently, the mean-based method exhibited a lower performance than the DDAM because the multipliers set in the DDAM were smaller than the multipliers  $V_{mean}$  used in the mean-based

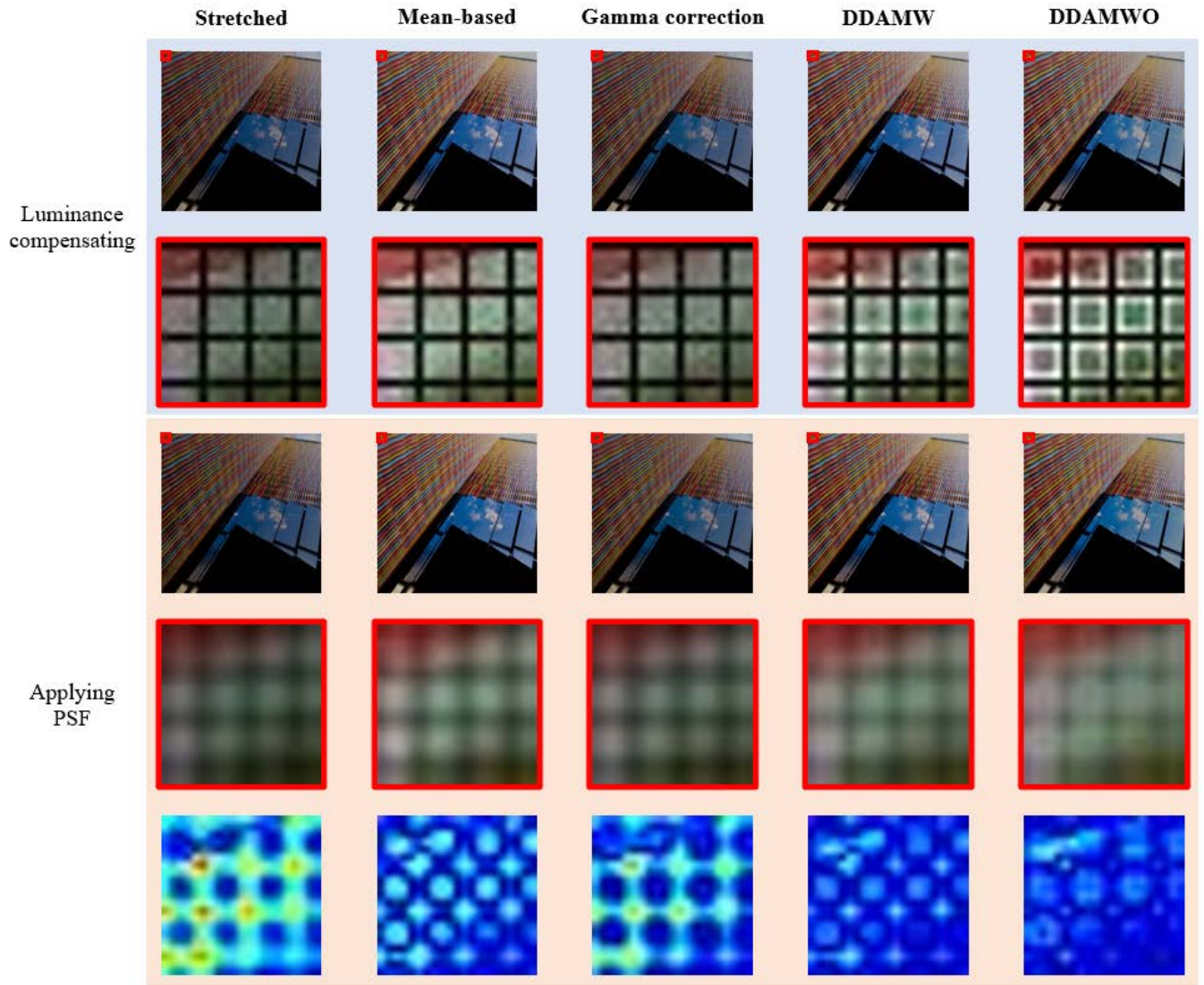


**FIGURE 6.** In the upper block (blue), the first row is the luminance compensated images applying different methods, and the second row shows the enlarged images for the red box in the images in the first row. In the lower block (red), the first row represents the images applying PSF to the compensated images using each method, and the second row shows the enlarged images for the red box in the first row. The third row shows the heatmaps between the ground truth images and the images to which PSF is applied for the red box. The stretch ratio is 5%, and the relative distance is 4.

method. Notably, when the stretch ratio was 33%, the PSNR of the DDAMWO was 14.962 dB, which is 0.434 dB lower than that of the DDAMW (15.396 dB). Because the mean of the compensation multipliers for the DDAMWO was larger than that for the DDAMW, saturation occurred more frequently. In addition, the luminance could not be accurately predicted because the value compensated by the DDAM was manually set considering the stretch ratio. Therefore, the DDAMWO could not adequately compensate for the luminance when the stretch ratio increased to 33% and exhibited a lower performance than that of the DDAMW in terms of the PSNR.

### C. RELATIVE DISTANCE

To compare the performance of the methods at different viewing distances, experiments were performed with relative

distances of 2, 3, and 4. As shown in Table 3, when the relative distance was set to 2 or 3, the performance order of the compensation methods was the same. Specifically, the zero-luminance pattern caused by the exposed substrate faded from most to least with the methods in the order of DDAMWO, DDAMW, mean-based method, and gamma correction method. Because the mean-based method and gamma correction method did not consider the exposed area of the substrate, the zero-luminance pattern was not faded when the PSF was applied, and the performance was inferior. In contrast, because the compensation multipliers of the DDAM were focused on the pixels near the zero-luminance pattern, the zero-luminance pattern was sufficiently compensated for, and higher performance was achieved. Notably, when the relative distance was 4, the PSNR of the DDAMWO was 17.765 dB, which is 0.123 dB lower than that of the DDAMW.

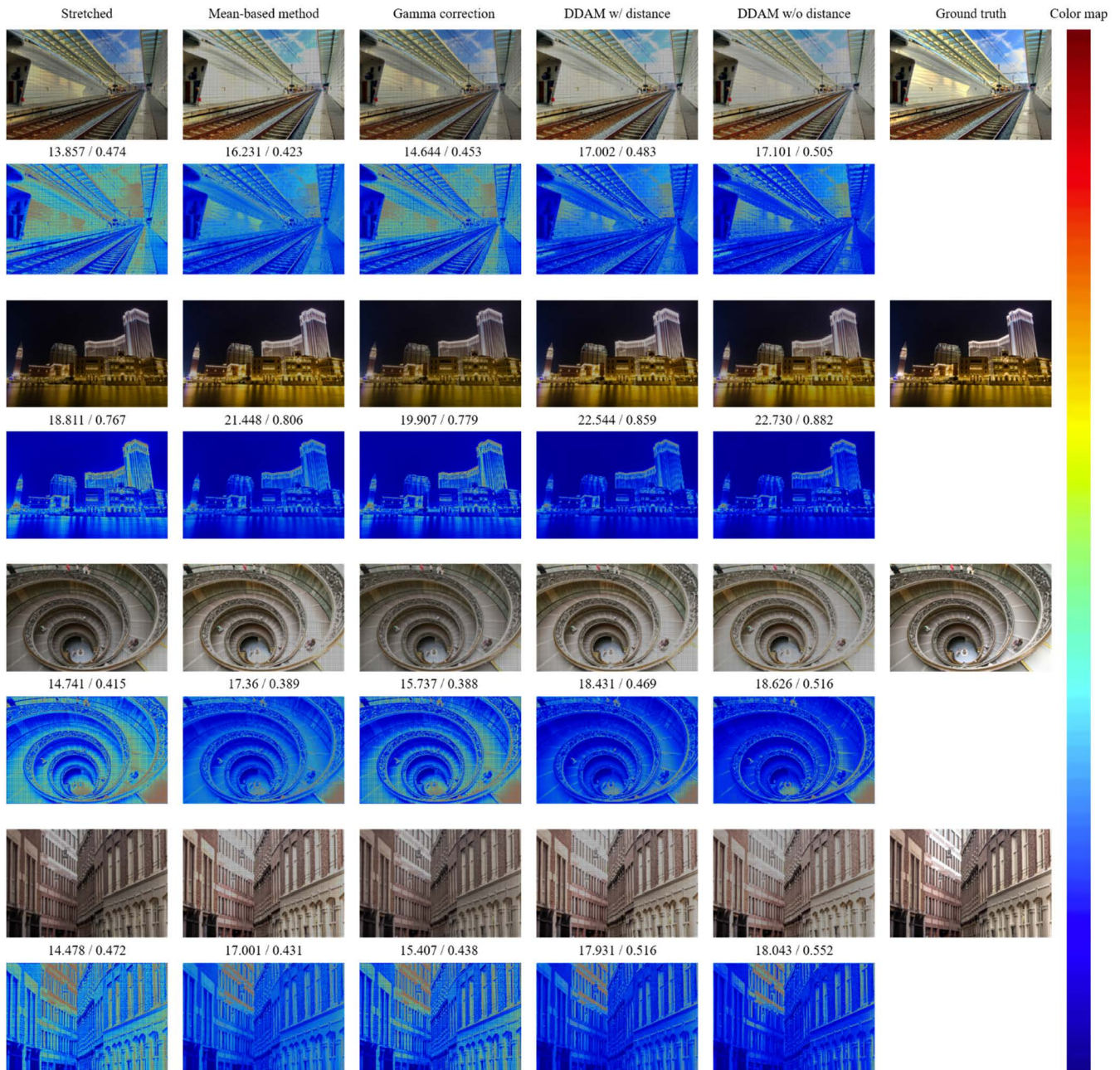


**FIGURE 7.** Comparison of the luminance reduction compensation methods: output images and heatmaps. The heatmap indicates the difference from the ground truth. The numbers on the left and right sides are the PSNR and SSIM, respectively. The stretch ratio is 20%, and the relative distance is 3.

**TABLE 2.** Average performance comparison of the luminance compensation methods according to the stretch ratio.

Stretch ratio	PSNR / SSIM			
	Mean-based	Gamma correction	DDAMW	DDAMWO
11%	17.811 / 0.579	17.285 / 0.562	18.751 / 0.620	<b>19.292 / 0.660</b>
20%	16.473 / 0.497	15.175 / 0.496	17.156 / 0.546	<b>17.251 / 0.566</b>
33%	15.319 / 0.485	13.014 / 0.494	<b>15.396 / 0.519</b>	14.962 / <b>0.537</b>

When the blur size was small, the DDAMWO could sufficiently compensate for the exposed area of substrate because the compensation multipliers for the pixels adjacent to the exposed substrates were large. In contrast, the DDAMW

did not sufficiently compensate for the exposed substrate because the compensation multipliers for pixels adjacent to the exposed area of substrate were small. Nevertheless, because the difference in the compensation multipliers of the



**TABLE 3.** Average performance comparison of the luminance compensation methods according to the relative distance.

Relative distance	PSNR / SSIM			
	Mean-based	Gamma correction	DDAMW	DDAMWO
2	15.327 / 0.466	14.571 / 0.468	15.962 / 0.506	<b>16.244 / 0.529</b>
3	16.875 / 0.533	15.340 / 0.529	17.452 / 0.577	<b>17.495 / 0.607</b>
4	17.400 / 0.561	15.563 / 0.555	<b>17.888 / 0.603</b>	17.765 / <b>0.628</b>

DDAMW was small, the resulting images due to the compensation were more natural than those of the DDAMWO when the blur size was large. Therefore, the DDAMWO exhibited the highest performance when the relative distance was 2 and 3, but the DDAMW outperformed the other methods when the relative distance was 4.

## V. CONCLUSION

In the implementation of stretchable displays, the zero-luminance pattern caused by exposed substrates leads to the optical underestimation of the luminance. We compared the results of the mean-based method, gamma correction method, and proposed DDAM in solving this problem. Because the mean-based method and gamma correction method do not consider the stretch ratios, the saturation problem occurs. The proposed DDAM, optimized for stretchable displays, can produce natural images by focusing the compensation effects on the pixels around the exposed substrate. In addition, we designed a simulator to conduct experiments for a high-PPI stretchable display. The performance of the different luminance compensation methods was compared by changing the stretch ratio and viewing distance. The results demonstrate that the DDAM method is highly suitable for stretchable displays because compared with the mean-based method and the gamma correction method, the DDAM achieved a PSNR that was 0.600 dB and 1.977 dB higher respectively. Additionally, the SSIM was also 0.055 and 0.057 higher, respectively.

## REFERENCES

- [1] J. H. Koo, D. C. Kim, H. J. Shim, T.-H. Kim, and D.-H. Kim, "Flexible and stretchable smart display: Materials, fabrication, device design, and system integration," *Adv. Funct. Mater.*, vol. 28, no. 35, Jul. 2018, Art. no. 1801834.
- [2] J. Wang and P. S. Lee, "Progress and prospects in stretchable electroluminescent devices," *Nanophotonics*, vol. 6, no. 2, pp. 435–451, Mar. 2017.
- [3] J.-H. Kim and J.-W. Park, "Intrinsically stretchable organic light-emitting diodes," *Sci. Adv.*, vol. 7, no. 9, Feb. 2021, Art. no. eabd9715.
- [4] S. Ye, A. R. Rathmell, Z. Chen, I. E. Stewart, and B. J. Wiley, "Metal nanowire networks: The next generation of transparent conductors," *Adv. Mater.*, vol. 26, no. 39, pp. 6670–6687, 2014.
- [5] J. Y. Lee, S. T. Connor, Y. Cui, and P. Peumans, "Solution-processed metal nanowire mesh transparent electrodes," *Nano Lett.*, vol. 8, no. 2, pp. 689–692, Jan. 2008.
- [6] J. Liang, L. Li, D. Chen, T. Hajagos, Z. Ren, S.-Y. Chou, W. Hu, and Q. Pei, "Intrinsically stretchable and transparent thin-film transistors based on printable silver nanowires, carbon nanotubes and an elastomeric dielectric," *Nature Commun.*, vol. 6, no. 1, pp. 1–10, Jul. 2015.
- [7] D. K. Choi, D. H. Kim, C. M. Lee, H. Hafeez, S. Sarker, J. S. Yang, H. J. Chae, G. W. Jeong, D. H. Choi, T. W. Kim, and S. Yoo, "Highly efficient, heat dissipating, stretchable organic light-emitting diodes based on a MoO<sub>3</sub>/Au/MoO<sub>3</sub> electrode with encapsulation," *Nature Commun.*, vol. 12, no. 1, pp. 1–11, May 2021.
- [8] T. C. Shyu, P. F. Damasceno, P. M. Dodd, A. Lamoureux, L. Xu, M. Shlian, M. Shtein, S. C. Glotzer, and N. A. Kotov, "A kirigami approach to engineering elasticity in nanocomposites through patterned defects," *Nature Mater.*, vol. 14, pp. 785–789, Jun. 2015.
- [9] L. Xu, T. C. Shyu, and N. A. Kotov, "Origami and kirigami nanocomposites," *ACS Nano*, vol. 11, no. 8, pp. 7587–7599, Aug. 2017.
- [10] J. Lyu, M. D. Hammig, L. Liu, L. Xu, H. Chi, C. Uher, T. Li, and N. A. Kotov, "Stretchable conductors by kirigami patterning of aramid-silver nanocomposites with zero conductance gradient," *Appl. Phys. Lett.*, vol. 111, no. 16, Oct. 2017, Art. no. 161901.
- [11] S. Ji, B. G. Hyun, K. Kim, S. Y. Lee, S. H. Kim, J. Y. Kim, M. H. Song, and J. U. Park, "Photo-patternable and transparent films using cellulose nanofibers for stretchable origami electronics," *NPG Asia Mater.*, vol. 8, no. 8, p. 299, Aug. 2016.
- [12] J. L. Silverberg, A. A. Evans, L. McLeod, R. C. Hayward, T. Hull, C. D. Santangelo, and I. Cohen, "Using origami design principles to fold reprogrammable mechanical metamaterials," *Science*, vol. 345, no. 6197, pp. 647–650, Aug. 2014.
- [13] N. Bowden, W. T. S. Huck, K. E. Paul, and G. M. Whitesides, "The controlled formation of ordered, sinusoidal structures by plasma oxidation of an elastomeric polymer," *Appl. Phys. Lett.*, vol. 75, no. 17, pp. 2557–2559, Oct. 1999.
- [14] N. Bowden, S. Brittain, A. Evans, J. Hutchinson, and G. Whitesides, "Spontaneous formation of ordered structures in thin films of metals supported on an elastomeric polymer," *Nature*, vol. 393, pp. 146–149, Mar. 1998.
- [15] W. Liu, J. Chen, Z. Chen, K. Liu, G. Zhou, Y. Sun, M.-S. Song, Z. Bao, and Y. Cui, "Stretchable lithium-ion batteries enabled by device-scaled wavy structure and elastic-sticky separator," *Adv. Energy Mater.*, vol. 7, no. 21, Nov. 2017, Art. no. 1701076.
- [16] O. H. Kwon, J. H. Oh, B. Gu, M. S. Jo, S. H. Oh, Y. C. Kang, J. K. Kim, S. M. Jeong, and J. S. Cho, "Porous SnO<sub>2</sub>/C nanofiber anodes and LiFePO<sub>4</sub>/C nanofiber cathodes with a wrinkle structure for stretchable lithium polymer batteries with high electrochemical performance," *Adv. Sci.*, vol. 7, no. 17, Sep. 2020, Art. no. 2001358.
- [17] W. Weng, Q. Sun, Y. Zhang, S. He, Q. Wu, J. Deng, X. Fang, G. Guan, J. Ren, and H. Peng, "A gum-like lithium-ion battery based on a novel arched structure," *Adv. Mater.*, vol. 27, no. 8, pp. 1363–1369, Feb. 2015.
- [18] R. Li, M. Li, Y. Su, J. Song, and X. Ni, "An analytical mechanics model for the island-bridge structure of stretchable electronics," *Soft Matter*, vol. 9, no. 35, pp. 8476–8482, Sep. 2013.
- [19] M. Zhang, H. Liu, P. Cao, B. Chen, J. Hu, Y. Chen, B. Pan, J. A. Fan, R. Li, L. Zhang, and Y. Su, "Strain-limiting substrates based on nonbuckling, prestrain-free mechanics for robust stretchable electronics," *J. Appl. Mech.*, vol. 84, no. 12, Dec. 2017.
- [20] C. A. Silva, J. Lv, L. Yin, I. Jeerapan, G. Innocenzi, F. Soto, Y. Ha, and J. Wang, "Liquid metal based Island-bridge architectures for all printed stretchable electrochemical devices," *Adv. Funct. Mater.*, vol. 30, no. 30, Jul. 2020, Art. no. 2002041.
- [21] K. Li, Y. Shuai, X. Cheng, H. Luan, S. Liu, C. Yang, Z. Xue, Y. Huang, and Y. Zhang, "Island effect in stretchable inorganic electronics," *Small*, vol. 18, no. 17, Apr. 2022, Art. no. 2107879.
- [22] I. E. Stewart, A. R. Rathmell, L. Yan, S. Ye, P. F. Flowers, W. You, and B. J. Wiley, "Solution-processed copper-nickel nanowire anodes for organic solar cells," *Nanoscale*, vol. 6, no. 6, pp. 5980–5988, Nov. 2014.
- [23] T.-H. Duong, H.-M. Hoang, and H.-C. Kim, "An investigation of electrical nickel deposition on copper nanowires-based electrodes," *Chem. Eng. Commun.*, vol. 207, no. 5, pp. 652–664, May 2020.
- [24] Y. Li, B. Wang, H. Hu, J. Zhang, B. Wei, and L. Yang, "Pseudo-biological highly performance transparent electrodes based on capillary force-welded hybrid AgNW network," *IEEE Access*, vol. 7, pp. 177944–177953, 2019.

- [25] J. Liang, L. Li, D. Chen, T. Hajagos, Z. Ren, S.-Y. Chou, W. Hu, and Q. Pei, "Intrinsically stretchable and transparent thin-film transistors based on printable silver nanowires, carbon nanotubes and an elastomeric dielectric," *Nature Commun.*, vol. 6, no. 1, pp. 1–10, Nov. 2015.
- [26] D. Kong, R. Pfattner, A. Chortos, C. Lu, A. C. Hinckley, C. Wang, W. Lee, J. W. Chung, and Z. Bao, "Capacitance characterization of elastomeric dielectrics for applications in intrinsically stretchable thin film transistors," *Adv. Funct. Mater.*, vol. 26, no. 26, pp. 4680–4686, Jul. 2016.
- [27] C. H. Yang, B. Chen, J. Zhou, Y. M. Chen, and Z. Suo, "Electroluminescence of giant stretchability," *Adv. Mater.*, vol. 28, no. 22, pp. 4480–4484, Jun. 2016.
- [28] F. M. Kochetkov, V. Neplokh, V. A. Mastaliev, S. Mukhangali, A. A. Vorob'ev, A. V. Uvarov, F. E. Komissarenko, D. M. Mitin, A. Kapoor, J. Eymery, N. Amador-Mendez, C. Durand, D. Krasnikov, A. G. Nasibulin, M. Tchernycheva, and I. S. Mukhin, "Stretchable transparent light-emitting diodes based on InGaN/GaN quantum well microwires and carbon nanotube films," *Nanomaterials*, vol. 11, no. 6, p. 1503, Jun. 2021.
- [29] D. H. Jiang, Y. C. Liao, C. J. Cho, L. Veeramuthu, F. C. Liang, T. C. Wang, C. C. Chueh, T. Satoh, S. H. Tung, and C. C. Kuo, "Facile fabrication of stretchable touch-responsive perovskite light-emitting diodes using robust stretchable composite electrodes," *ACS Appl. Mater. Interfaces*, vol. 12, no. 12, pp. 14408–14415, Dec. 2020.
- [30] B. Jang, S. Won, J. Kim, J. Kim, M. Oh, H. Lee, and J. Kim, "Auxetic meta-display: Stretchable display without image distortion," *Adv. Funct. Mater.*, vol. 32, no. 22, May 2022, Art. no. 2113299.
- [31] J. H. Koo, D. C. Kim, H. J. Shim, T.-H. Kim, and D.-H. Kim, "Flexible and stretchable smart display: Materials, fabrication, device design, and system integration," *Adv. Funct. Mater.*, vol. 28, no. 35, Aug. 2018, Art. no. 1801834.
- [32] B.-S. Bae, G.-M. Choi, Y. H. Kim, Y. H. Kim, and J.-H. Ko, "Flexible hard coating (Flex9H) for foldable display cover plastic film," in *SID Symp. Dig. Tech. Papers*, vol. 48, no. 1, May 2017, pp. 215–217.
- [33] G.-M. Choi, J. Jin, D. Shin, Y. H. Kim, J.-H. Ko, H.-G. Im, J. Jang, D. Jang, and B.-S. Bae, "Flexible hard coating: Glass-like wear resistant, yet plastic-like compliant, transparent protective coating for foldable displays," *Adv. Mater.*, vol. 29, no. 19, May 2017, Art. no. 1700205.
- [34] Y.-C. Jeong, "P-212: Late-news poster: Flexible cover window for foldable display," in *SID Symp. Dig. Tech. Papers*, vol. 49, no. 1, May 2018, pp. 1921–1924.
- [35] K. Hu, B. Yuan, Y. Li, P. Dang, and X. Huang, "Technical challenge and improvement method of foldable display during cycle bending test," in *SID Symp. Dig. Tech. Pap.*, vol. 49, 2018, pp. 409–410.
- [36] C. Lu and X. Chen, "All-temperature flexible supercapacitors enabled by anti-freezing and thermal-stable hydrogel electrolyte," *Nano Lett.*, vol. 20, no. 3, pp. 1907–1914, Mar. 2020.
- [37] A. Das, S. Sengupta, J. Deka, A. M. Rather, K. Raidongia, and U. Manna, "Synthesis of fish scale and lotus leaf mimicking, stretchable and durable multilayers," *J. Mater. Chem. A*, vol. 6, no. 33, pp. 15993–16002, 2018.
- [38] J. H. Lee, M. H. Myung, M. J. Baek, H.-S. Kim, and D. W. Lee, "Effects of monomer functionality on physical properties of 2-ethylhexyl acrylate based stretchable pressure sensitive adhesives," *Polym. Test.*, vol. 76, pp. 305–311, Jul. 2019.
- [39] S. Zhou and L. Jiang, "Modern description of Rayleigh's criterion," *Phys. Rev. A, Gen. Phys.*, vol. 99, no. 1, Jan. 2019, Art. no. 013808.
- [40] R. T. Held, E. A. Cooper, J. F. O'Brien, and M. S. Banks, "Using blur to affect perceived distance and size," *ACM Trans. Graph.*, vol. 29, no. 2, pp. 1–16, Mar. 2010.
- [41] K. Noland and L. Truong, "A survey of U.K. Television viewing conditions," *BBC Res. Develop. White Paper*, vol. 287, pp. 1–58, Jan. 2015.
- [42] K.-K. Shieh and M.-T. Chen, "Effects of screen color combination, work-break schedule, and workplace on VDT viewing distance," *Int. J. Ind. Ergonom.*, vol. 20, no. 1, pp. 11–18, Jul. 1997.
- [43] J.-B. Huang, A. Singh, and N. Ahuja, "Single image super-resolution from transformed self-exemplars," in *Proc. IEEE Conf. Comput. Vis. Pattern Recognit.*, Jun. 2015, pp. 5197–5206.



**SUNG-HOON JUNG** received the B.S. degree in electronics engineering from Sogang University, Seoul, South Korea, in 2022, where he is currently pursuing the M.S. degree in electronics engineering. His current research interests include image processing, computer vision, and deep learning.



**JUNG-HYUN KIM** received the B.S. degree in electronics engineering from Kangwon National University, Chuncheon, Gangwon, South Korea, in 2020. He is currently pursuing the M.S. degree in electronics engineering with Sogang University, Seoul, South Korea. His current research interests include image processing, computer vision, and deep learning.



**SUK-JU KANG** (Member, IEEE) received the B.S. degree in electronics engineering from Sogang University, South Korea, in 2006, and the Ph.D. degree in electrical and computer engineering from the Pohang University of Science and Technology, in 2011. From 2011 to 2012, he was a Senior Researcher at LG Display, where he was a Project Leader for resolution enhancement and multiview 3D system projects. From 2012 to 2015, he was an Assistant Professor of electrical engineering at Dong-A University, Busan. He is currently a Professor of electronic engineering with Sogang University. His current research interests include image analysis and enhancement, video processing, multimedia signal processing, circuit design for display systems, and deep learning systems. He was a recipient of the IEIE/IEEE Joint Award for young IT engineer of the year, in 2019.

...